A robust control strategy for virtual coupling train platoons

by

X. Dong

as a additional graduation project
at the Delft University of Technology,
defended on Monday January 23, 2023 at 13:00 PM.

Student number:	5464099	
Track:	Transport & Planning (TP)	
Project duration:	September 12, 2023 – January 23, 2023	
Thesis committee:	Prof. dr. R. M. P. (Rob) Goverde	TU Delft, supervisor
	A. (Alex) Cunillera,	TU Delft, supervisor

TU Delft

Abstract

This paper presents a train robust control method to optimize train operation based on the concept virtual coupling on train platoon. This approach is inspired by the recent development of platoon control for autonomous vehicles, and it is hoped that this platoon control can be applied to railway transportation. We use a decentralized model predictive control (MPC) to control leading train and followers together. To solve the complexity minimax objective function, we reformulated objective function as a minimization problem subject to linear matrix inequalities (LMIs). We defined four weight parameters to evaluate the model. Simulation result indicated that based on the premise of platoon stability, increase the performance parameters to obtain an optimal solution. We show that after the virtual coupling of less than two minutes, the gap distance between two consecutive trains is reduced and the capacity is increased while ensuring safey.

Keywords— Robust control, Train platoon, Virtual coupling, Train control system

1 Introduction

Railway transport demand continues growing, and the capacity has become an important factor in promoting the development of railway transportation. Railway signalling system designed to convey information to drivers to control train movement in a safe manner. The capacity offered by conventional signaling systems is very limited. Fixed block and moving block are two main types of signalling system. The fixed block system divides the railway network into fixed blocks which are separated by signals. A train is not allowed to enter a given track section before the preceding train has cleared it. Moving block does not require traditional track-clear detection for determining train position. Instead, it relies on continuous two-way digital communication between each controlled train and a wayside control centre and Train Integrity Monitoring. The train's occupying track part becomes the moving block in which no other train can enter. Both signalling systems imply huge separations between trains, lowering significantly the available capacity. This conservative operation causes a large distance gap between trains. In reality, focus on the relative braking distance of consecutive trains, the distance gap between two consecutive trains can be reduced. So a closer communication between trains can help further minimizing separations.

Virtual Coupling (VC) is a concept that expands moving block signalling by relying on the assumption that trains communicate with each other via a Vehicle-to-Vehicle (V2V) radio layer, allowing to reduce the train separation further than less of the absolute braking distance. Trains can hence form a platoon following each other at a relative braking distance as function of their speed difference or even travel in platoons where they move synchronously at a short distance from each other (Quaglietta et al., 2022). ETCS Level 3 is a first step towards VC as VC needs the components developed for ETCS Level 3. Virtual coupling enables the virtually combining and splitting of vehicles on the move by controlling the gap between the vehicles without any mechanical coupling, which is one of the technologies for increasing the transport capacity and enhancing operational efficiency (Park, Lee, & Eun, 2022).

Virtual coupling technology presents the following advantages. First, it increases the line capacity by reducing the departure interval and the headways. Second, in VC, trains can be coupled and decoupled dynamically according to the service needs and respecting the safety requirements, which allows trains to be more flexible in adapting to complex rail transport service tasks.

In order to virtually couple two trains, the following two points are very important. The first one is the use of moving block system, which is based on the fact that the trains continuously calculate and communicate their exact position, speed and train integrity to the wayside

equipment distributed along the line, these continuous data transmission via Global System for Mobile Communications − Railway (GSM-R) with the Radio-Block Center (RBC) give the required information to trains. That allows the calculation of the track segment to be potentially occupied by the train, giving the movement authority and continuously adjust their speeds while ensuring safety and comfort. The moving block system makes the assumption that the consecutive trains on the same track must be separated by an absolute braking distance and an extra safety margin to ensure that each train is capable of braking and stopping before reaching the last known position of the train ahead at any time. The other is high reliability and low time-delay V2V communication technology. Trains are virtually-coupled via V2V communication, sharing information with other trains in platoon and radio-based Vehicle-to-Infrastructure (V2I) communication with the RBC reporting train position. On the basis of the information received from the trains within the convoy, the on-board system is responsible for the train speed to keep a desired distance to the predecessor, allowing the follower to pursue the leader train in a safe way (Zhang, Yang, Zhang, & Huang, 2022).

Quaglietta (2019) proposed a mode of train platoon operation in which the leading train of a platoon moves under ETCS Level 3, a train getting closer to preceding train will switch its control from ETCS Level 3 to VC. In such a case, the train communicates to the preceding train by means of the V2V communication speed, position, acceleration. This information is used by the following train's on-board subsystem to compute the relative braking distance which let the train move at the same speed of the leader. For controlling the platoons, Park et al.(2020) assume that the leading train runs with speed control and that the following train keeps the target distance gap with the leading train using a gap controller. Therefore, in Park et al., (2020) model, all trains must equip both a velocity controller and gap controller to select the appropriate controller according to one's role in the convoy.

This paper has the objective of implementing an approach from connected automated vehicles (road traffic) of the robust platooning control to a virtual-coupled train platoon. The research question of this paper can then be stated as follows:

What changes are needed to a robust platoon controller to optimize virtual coupling?

Different from the traditional train operation, VC train platoon maintain a smaller distance gap between trains, therefore, the control of train operation needs to be more advanced and accurate. MPC (model predictive control) is a control algorithm that relies on the iterative solution of an optimal control problem based on the predicted state to compute a control input at each sampling. Felez et al.∼(2019) use a decentralized MPC framework for each train participating in a convoy formation. They pointed out that there are two possible control architectures for VC. The first one is centralized VC, in which trains cooperate in order to optimize the overall convoy strategy. The second control architecture is decentralized VC, in which each train optimizes its own strategy given the movement estimation of the preceding train. Compared to the decentralized controller, the centralized controller focuses more on the whole system optimum rather than individual local optimum.

Chen et al.(2018) designed a robust platooning control strategy for connected automated vehicles (CAVs). A centralized control method is used to make cooperation driving system stable under time delay or some uncertainties happen. The control process is that the leader of a CAV platoon collects information from followers then computes the desired acceleration for all controlled vehicles. After this calculation, broadcasts the information to followers to make them drive at the right acceleration to meet the desired distance gap.

The vehicle dynamics in train operation and road traffic use similar variables and parame-

ters such as acceleration, headway and other basic parameters, but some factors that affect the robust platooning control approaching model are still different. For example the way to position vehicles and the impact of the track geometry on the train dynamics/platoon. So we assess some of the similarities as well as the differences to identify possibilities for model improvement and differences between railway operation and road traffic for the robust control operation.

The position of vehicles is an important factor to influence the model accuracy. The accurate feedback information on positions of controlled vehicles can be obtained via V2V communication and on-board sensors like odometers or GNSS (Global Navigation Satellite System), but is subject to a fixed feedback delay. But for VC in railways, in addition to positioning feedback delay, VC headways will be dependent on train positioning system precision (e.g. odometer error or satellite positioning resolution in future generation ERTMS) which has an influence on the entity of safe margins (i.e. minimum/maximum safe rear/front end), and on the V2V connection performance (including bandwidth and stability) together with the availability of appropriate sensors/radars. (Di Meo et al., 2019)

Another difference between railway operation and road traffic is that the impact of track geometry on train operation is more obvious. Quaglietta et al.(2020) developed a multi-state train-following model that overcomes limitation of car-following model by considering line resistances due to track gradient and curvature. Quaglietta et al.(2022) proposed five safety-critical risk factors for VC that need to be determined. These are train positioning error, communication update delays, train control delays, emergency braking application of the leader train and exogenous factors, and a dynamic safety margin is defined as the sum of these five factors. By calculating the sensitivity indexes for flat track and with the actual track with gradients, the results shows that the following train's braking rate is the most influential parameter to VC capacity, means significant changes in train operation due to track geometry. Barney et al.(2001) also indicated that one of the influencing factors of braking distance is the track gradient the train travels over from when the brakes are commanded to where the front of the train stops. So for a VC platoon on a line with gradients, the controller should continuously adjust the desired gap distance as the gradient changes.

Although railway operations share many motion similarities with road traffic, differences are still shown in terms of train length, mass, sensor delay and gradient effects. In this article we using the concept of virtual coupling and MPC, develops a control system that reduces distance between trains and combine several trains into one train platoon while guaranteeing safe separation between two consecutive trains.

The contribution of this paper is we defined a robust MPC model for train platoon. And while realizing the train VC, by adjusting the weight parameters, balance the entire virtual coupling process in terms of smoothness, convergence time, comfort and other aspects makes the whole optimization process optimal.

The remainder of this paper is organized as follows. Section II defines the state prediction problem and present a robust MPC train dynamics model. Section III formulates the nonlinear MPC developed for virtual coupling including the design assumption, the cost function and the different constraints that have been considered. Section IV presents a method to makes the optimization process achievable by rewriting minimax problem as a minimization problem. Section V presents the different weight tests, simulations and results. Finally, Section VI includes the conclusions of this work.

Notation: For a vector x and positive-definite matrix ξ, $||x||_{\xi}^{2} = x^{T}\xi x$.

2 Dynamics models

This section presents a robust MPC train dynamics model for state prediction for VC train platoon considering actuator lag.

2.1 Single train dynamics model

Consider a VC train platoon with one leader and N followers, propose a dynamics model for a train n with x_n, v_n, a_n and l_n representing the location, speed, actual acceleration and train length of the subject train n. The leading train is train $n = 0$ and it aims to track a reference speed v_{ref}. As shown in Figure 1, s_n is the distance gap between train n and its preceding train $n-1$, $s_n = x_{n-1} - l_{n-1} - x_n$. We define the distance gap error Δs_n as the deviation between the distance gap s_n and the desired distance gap s_n^d to the preceding train $n-1$ for train n, i.e. $\Delta s_n = s_n - s_n^d$. We define the desired distance gap $s_n^d = v_n t^d + s_{min}$, where s_{min} is the minimum distance gap to be kept between trains, t^d is the desired time gap between trains to control the desired distance gap. And the relative speed $\Delta v_n = v_{n-1} - v_n$ $(n \geq 1)$ is the speed difference to the preceding train.

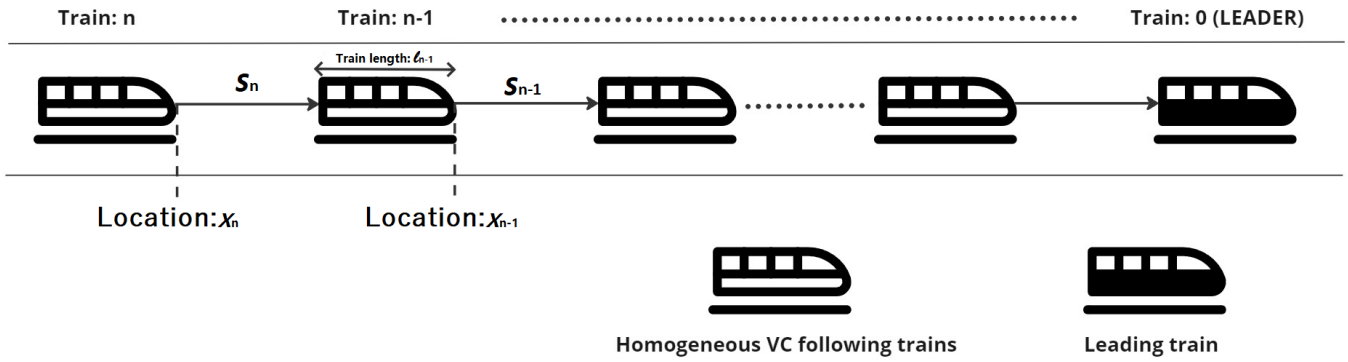

Figure 1: Train platooning formation

For a single train $n \geq 1$ in VC platoon, the system state Z_n is described by the gap error Δs_n, relative speed Δv_n and acceleration a_n.

$$Z_n = (\Delta s_n, \Delta v_n, a_n)^T \tag{1}$$

The control variable is defined as u_n, which is the desired acceleration of train n. Following a third-order derivative formula, the system dynamics is described by Equation 2.

$$\frac{\mathrm{d}}{\mathrm{d}t} Z_n = \frac{\mathrm{d}}{\mathrm{d}t} \begin{pmatrix} \Delta s_n \\ \Delta v_n \\ a_n \end{pmatrix} = \frac{\mathrm{d}}{\mathrm{d}t} \begin{pmatrix} x_{n-1} - l_{n-1} - x_n - s_n^d \\ v_{n-1} - v_n \\ a_n \end{pmatrix} = \begin{pmatrix} \Delta v_n - a_n \cdot t^d \\ a_{n-1} - a_n \\ \frac{u_n - a_n}{\tau_n^A} \end{pmatrix} = f(Z_n, u_n) \tag{2}$$

In Equation 2, $\frac{u_n - a_n}{\tau_n^A}$ is the dynamics of the acceleration means the control rate of the acceleration (Chen et al., 2018). And the actuator lag τ_n^A is considered here uncertain, but with known upper and lower bounds.

$$f(Z_n, u_n) = A_n Z_n + B_n u_n + \begin{pmatrix} 0 \\ 1 \\ 0 \end{pmatrix} a_{n-1} \tag{3}$$

where,

$$A_n = \begin{bmatrix} 0 & 1 & -t^d \\ 0 & 0 & -1 \\ 0 & 0 & -\frac{1}{\tau_n^A} \end{bmatrix}; B_n = \begin{bmatrix} 0 \\ 0 \\ \frac{1}{\tau_n^A} \end{bmatrix}$$

And $\begin{pmatrix} 0 \\ 1 \\ 0 \end{pmatrix} a_{n-1}$ is an exogeneous disturbance to the train system, which is the actual acceleration of the preceding train.

We model the dynamics of the leading train in a similar way to the followers. The location, speed, acceleration and train length of the leader train are x_0, v_0, a_0 and l_0, respectively. No distance gap is needed because there is no preceding train. We assume that the target speed of the leading train is a constant reference speed (v_{ref}). So the relative speed for the leading train is the error between the reference speed and the speed of the leader train $\Delta v_0 = v_{ref} - v_0$. And the state for the first train is:

$$\frac{d}{dt} Z_0 = \frac{d}{dt} \begin{pmatrix} \Delta v_0 \\ a_0 \end{pmatrix} = \begin{pmatrix} -a_0 \\ \frac{u_0 - a_0}{\tau_0^A} \end{pmatrix} = f(Z_0, u_0) \tag{4}$$

where,

$$A_0 = \begin{bmatrix} 0 & -1 \\ 0 & -\frac{1}{\tau_0^A} \end{bmatrix}; B_0 = \begin{bmatrix} 0 \\ \frac{1}{\tau_0^A} \end{bmatrix}$$

2.2 Platoon dynamics model

To describe the platoon dynamic model, we rewrite Equation 2 and Equation 4 as a single linear matrix system by considering the state of the whole convoy of trains Z. The platoon state is defined as $Z = (\Delta v_0, a_0, \Delta s_1, \Delta v_1, a_1, ..., \Delta s_N, \Delta v_N, a_N)^T$, the control variable is defined as $U = (u_0, u_1, u_2, ..., u_N)^T$. The system dynamics model for a VC platoon with N followers can be expressed as:

$$\frac{\mathrm{d}}{\mathrm{d}t} Z = A \cdot Z + B \cdot U \tag{5}$$

where,

$$A = \begin{pmatrix} [& A_0 &]^{2\times 2} & & \cdots & 0 & \\ & [& A_1 &]^{3\times 4} & & \vdots & \\ & & [& A_2 &]^{3\times 4} & & \\ & \vdots & & & \ddots & & \\ & 0 & \cdots & & [& A_N &]^{3\times 4} \end{pmatrix}, B = \begin{pmatrix} B_0 & \cdots & \cdots & \cdots & 0 \\ \vdots & B_1 & & & \vdots \\ \vdots & & B_2 & & \vdots \\ \vdots & & & \ddots & \vdots \\ 0 & \cdots & \cdots & \cdots & B_N \end{pmatrix}$$

where,

$$A_0 = \begin{bmatrix} 0 & -1 \\ 0 & -\frac{1}{\tau_0^A} \end{bmatrix}; A_i = \begin{bmatrix} 0 & 0 & 1 & -t^d \\ 1 & 0 & 0 & -1 \\ 0 & 0 & 0 & -\frac{1}{\tau_i^A} \end{bmatrix}, i = 1, 2, 3, ..., N;$$

$$B_0 = \begin{bmatrix} 0 \\ \frac{1}{\tau_0^A} \end{bmatrix}; B_i = \begin{bmatrix} 0 \\ 0 \\ \frac{1}{\tau_i^A} \end{bmatrix}, i = 1, 2, 3, ..., N;$$

And now the exogenous disturbance term from Equation 3 is included in the sub-matrices A_i.

3 Design of robust controller for platoon operation

3.1 Design assumptions

The homogeneous VC platooning controller is designed based on the following assumptions:

- The VC trains are homogeneous. They have the same train length, desired acceleration boundary, speed limits and the same actuator lag $\tau^A = \tau_0^A = ... = \tau_N^A$.
- The accurate feedback information on positions, speeds and actual accelerations of controlled vehicles can be obtained via on-board sensors, RBCs and V2V communication.
- The controller apples the control command at regular intervals of time Δt. The robust MPC algorithm calculates this for the next M intervals of time, but only the first one is implemented at each iteration.
- The uncertainty in the dynamics of the trains in the platoon is made explicit in the matrices A and B, which depend on an uncertain parameter τ^A. In the model, τ^A is a constant actuator lag with $\tau^A \in [\alpha, \beta]$, $(0 < \alpha < \beta)$.
- The train tracks are straight and flat without gradient.

3.2 Platooning control formulation

3.2.1 Min-Max model predictive control problem

The designed controller minimize a cost function $J(Z, U)$ over a time horizon under the worst case, which express by Chen et al. as:

$$\min_{u[t_0,t_0+t_h]} \max_{[A,B]\in\Omega} J(Z,U) = \min_{u[t_0,t_0+t_h]} \max_{[A,B]\in\Omega} \sum_{j=t_0}^{t_0+t_h} J(Z(j),U(j)) \tag{6}$$

where Ω is a polytope defined by all the possible values of the uncertain matrices A and B, which depend on the value of the uncertain parameter τ^A. $\Omega = \{[A,B] : \alpha \leq \tau^A \leq \beta\}$. t_h is the prediction horizon.

The main goal is to find the best control policy in the interval $[t_0, t_0 + t_h]$ that will work for any of the possible values of τ_A. This problem is subject to the dynamics of the platoon described in Equation 5 and the following constraints.

3.2.2 Constraints

1. Speed constraints

   The speed of all trains should be non-negative and must not exceed the the speed limit v_{max}, i.e. $v_n \in [0, v_{max}], n = 0, 1, 2, ..., N$.

   To link the speed constraint with the dynamic system state Z and control U, v_n needs to be rewritten as a function of the variables in Z.

   - For $v_n \leq v_{max}$:

   $$v_{max} - v_{ref} + \sum_{i=0}^{n} \Delta v_i \geq 0, n = 0, 1, 2, ..., N; \tag{7}$$

   - For $v_n \geq 0$:

   $$v_{ref} - \sum_{i=0}^{n} \Delta v_i \geq 0, n = 0, 1, 2, ..., N; \tag{8}$$

2. Gap constraint

   The gap constraint shows that the real gap distance s_n to train n and preceding train $n-1$ for $n \geq 1$ should be larger or equal to the minimum distance gap s_{min} and less or equal to the maximum distance gap s_{max} (define $s_{max} = H + s_{min}$ which H is a sufficiently large fixed value), that is $s_{min} \leq s_n \leq s_{max}$. Again, this should be rewritten as a function of Δs_n and Δv_n. After rewriting, the gap constraint is expressed as:

$$\Delta s_n - t^d \cdot \left(\sum_{i=0}^{n} \Delta v_i \right) + t^d \cdot v_{ref} \geq 0, n = 1, 2, ..., N; \tag{9}$$

$$\Delta s_n - t^d \cdot \left(\sum_{i=0}^{n} \Delta v_i \right) + t^d \cdot v_{ref} - H \leq 0, n = 1, 2, ..., N; \tag{10}$$

3. Acceleration constraint

   The acceleration of each train $a_n \in [a_{min}, a_{max}]$. The acceleration constraint can be written directly as :

$$a_{min} \leq a_n \leq a_{max}, n = 0, 1, 2, ..., N; \tag{11}$$

4. Control constraint

   In addition to three state constraints, control variables are also constrained by the maximum and minimum accelerations that can be achieved, which is the same as the acceleration constraint. For control vector $U = (u_0, u_1, u_2, ..., u_N)^T$.

$$a_{min} \leq u_n \leq a_{max}, n = 0, 1, 2, ..., N; \tag{12}$$

3.2.3 Cost function

The cost function J (Equation 13) is related to performance, platoon stability, comfort and energy consumed measured by s_i, v_i, a_i, u_i respectively, where c_1, c_2, c_3 and c_4 are their associated weight parameters.

$$J(Z, U) = c_1 \cdot \sum_{i=1}^{N} (\Delta s_i)^2 + c_2 \cdot \sum_{i=1}^{N} (\Delta v_i)^2 + c_3 \cdot \sum_{i=1}^{N} (a_i)^2 + c_4 \cdot \sum_{i=1}^{N} (u_i)^2 \tag{13}$$

The performance cost term implies that it tries to minimize the distance gap to reduce the convergence time. The stability cost term makes the relative speed between followers and preceding trains smaller to keep the following behavior more stable in VC platoon. The energy cost penalizes large values of desired acceleration to save energy by making the train accelerate/decelerate process more smoothly. Also smooth acceleration/deceleration can make the train service more comfortable for passengers. The controller regulates platoon desired accelerations over a time horizon to minimize this cost function subject to speed limits, desired acceleration constraint and minimal gap distance (Equation 7 - Equation 12).

3.2.4 Time discretization

Since we aim to apply minimax MPC to calculate and update the control policy U at regular intervals of time Δt, we discretize the minimax MPC problem defined by Equation 6 - Equation 13, and we will solve the resulting robust problem until time goes to infinity, starting from $t_0 = 0$, and then apply the calculated optimal control policy from t_0 to $t_1 = t_0 + \Delta t$. Then, we repeat this starting from t_1, apply the resulting robust optimal policy from t_1 to t_2 and repeat this iterative process indefinitely. So the continuous time should be discretized. Starting from time $t_0 = 0$, the time is divided in regular intervals $(t_0, t_1, ...)$ with time step (control

update time) Δt i.e. $t_{k+1} = t_k + \Delta t$. To simplify the notation, we drop the t of the t_k, so $Z(k) = Z(t_k), k = (0, 1, ...)$.

- For Equation 5,

$$Z(k+1) = \overline{A}Z(k) + \overline{B}u(k) \tag{14}$$

where,

$$\overline{A} = \Delta t \cdot A + I, \overline{B} = \Delta t B$$

- For Equation 7 and Equation 8,

$$v_{max} - v_{ref} + \sum_{i=0}^{n} \Delta v_i(k) \geq 0, n = 0, 1, 2, ..., N; k = 0, 1, ...; \tag{15}$$

$$v_{ref} - \sum_{i=0}^{n} \Delta v_i(k) \geq 0, n = 0, 1, 2, ..., N; k = 0, 1, ...; \tag{16}$$

- For Equation 9 and Equation 10,

$$\Delta s_n(k) - t^d \cdot (\sum_{i=0}^{n} \Delta v_i(k)) + t^d \cdot v_{ref} \geq 0, n = 1, 2, ..., N; k = 0, 1, ...; \tag{17}$$

$$\Delta s_n(k) - t^d \cdot (\sum_{i=0}^{n} \Delta v_i(k)) + t^d \cdot v_{ref} - H \leq 0, n = 1, 2, ..., N; k = 0, 1, ...; \tag{18}$$

- For Equation 11 and Equation 12,

$$\begin{pmatrix} I \\ -I \end{pmatrix} \cdot a(k) \leq \begin{pmatrix} a_{max} \\ -a_{min} \end{pmatrix}, k = 0, 1, ...; \tag{19}$$

$$\begin{pmatrix} I \\ -I \end{pmatrix} \cdot u(k) \leq \begin{pmatrix} a_{max} \\ -a_{min} \end{pmatrix}, k = 0, 1, ...; \tag{20}$$

where $a = (a_0, ..., a_N)$, $u = (u_0, ..., u_N)$ and I is identity matrix.

- For the cost function Equation 13,

$$J(k) = \sum_{i=0}^{\infty} Z(k+i)^T L Z(k+i) + u(k+i)^T R u(k+i), k = 0, 1, ...; \tag{21}$$

where L and R are weighting matrices, i.e.

$$L = \begin{pmatrix} c_2 & & \cdots & & 0 \\ & c_3 & & & \\ & & c_1 & & \\ \vdots & & & c_2 & \vdots \\ & & & & c_3 \\ & & & & & \ddots \\ 0 & & \cdots & & & & c_3 \end{pmatrix}^{(3\times N+2)\times(3\times N+2)}$$

$$, R = \begin{pmatrix} c_4 & & 0 \\ & \ddots & \\ 0 & & c_4 \end{pmatrix}^{(N+1)\times(N+1)}$$

3.2.5 Constraint combination

Then we combine all constraints into two parts: state constraints and control constraint.

State constraints

For speed constraints:

$$\underline{\psi}_1 = (v_{ref} - v_{max}) \begin{bmatrix} 1 \\ \vdots \\ 1 \end{bmatrix}^{(N+1)\times 1} \leq \psi_1 Z \leq v_{ref} \begin{bmatrix} 1 \\ \vdots \\ 1 \end{bmatrix}^{(N+1)\times 1} = \overline{\psi}_1 \tag{22}$$

with,

$$\psi_1 = \begin{bmatrix} [1 & 0] & 0 & 0 & 0 & 0 & 0 & 0 & \cdots & & 0 \\ [1 & 0] & [0 & 1 & 0] & 0 & 0 & 0 & \cdots & & 0 \\ [1 & 0] & [0 & 1 & 0] & [0 & 1 & 0] & \cdots & & 0 \\ \vdots & \vdots & & \vdots & & & \vdots & & \ddots & & \\ [1 & 0] & [0 & 1 & 0] & [0 & 1 & 0] & \cdots & [0 & 1 & 0] \end{bmatrix}$$

For gap constraints:

$$\underline{\psi}_2 = (-t^d \cdot v_{ref}) \begin{bmatrix} 1 \\ \vdots \\ 1 \end{bmatrix}^{(N+1)\times 1} \leq \psi_2 Z \leq (H - t^d \cdot v_{ref}) \begin{bmatrix} 1 \\ \vdots \\ 1 \end{bmatrix}^{(N+1)\times 1} = \overline{\psi}_2 \tag{23}$$

with,

$$\psi_2 = \begin{bmatrix} [-t^d & 0 & 1 & -t^d & 0] & 0 & 0 & 0 & 0 & & & \cdots & & 0 \\ -t^d & 0 & 0 & [-t^d & 0 & 1 & -t^d & 0] & 0 & & & \cdots & & 0 \\ \vdots & & & & \vdots & & & & \ddots & & & & & \\ -t^d & 0 & 0 & -t^d & 0 & 0 & -t^d & \cdots & & [-t^d & 0 & 1 & -t^d & 0] \end{bmatrix}$$

For acceleration constraints:

$$\underline{\psi}_3 = a_{min} \begin{bmatrix} 1 \\ \vdots \\ 1 \end{bmatrix}^{(N+1)\times 1} \leq \psi_3 Z \leq a_{max} \begin{bmatrix} 1 \\ \vdots \\ 1 \end{bmatrix}^{(N+1)\times 1} = \overline{\psi}_3 \tag{24}$$

with,

$$\psi_3 = \begin{bmatrix} [0 & 1] & 0 & 0 & 0 & 0 & & \cdots & & & 0 \\ 0 & 0 & [0 & 0 & 1] & 0 & & \cdots & & & 0 \\ 0 & 0 & 0 & 0 & 0 & [0 & 0 & 1] & \cdots & & 0 \\ \vdots & & & \vdots & & & & & \ddots & & \\ 0 & 0 & 0 & 0 & 0 & & \cdots & & [0 & 0 & 1] \end{bmatrix}$$

In this way, the state constraint can be expressed as:

$$-\underline{\psi} \leq \psi Z \leq \overline{\psi} \tag{25}$$

with,

$$\underline{\psi} = \begin{bmatrix} \underline{\psi}_1 \\ \underline{\psi}_2 \\ \underline{\psi}_3 \end{bmatrix}, \ \psi = \begin{bmatrix} \psi_1 \\ \psi_2 \\ \psi_3 \end{bmatrix}, \ \overline{\psi} = \begin{bmatrix} \overline{\psi}_1 \\ \overline{\psi}_2 \\ \overline{\psi}_3 \end{bmatrix}$$

Control constraint

$$-\underline{u} = a_{min} \begin{bmatrix} 1 \\ \vdots \\ 1 \end{bmatrix}^{(N+1)\times 1} \leq u \leq a_{max} \begin{bmatrix} 1 \\ \vdots \\ 1 \end{bmatrix}^{(N+1)\times 1} = \overline{u} \tag{26}$$

4 Robust predictive control

In this section, we use a robust control algorithm to rewrite the minimax problem as a minimization problem subject to several LMIs constraints, following the approach introduced by Ding et al. (2004).

After time discretization, the dynamic model is reformulated to a discrete time model shown in Equation 14 with the constraints (15) - (20). With the combination of state and control constraints (25) and (26), the state and control constraints are expressed as:

$$-\underline{u} \leq u(k+i) \leq \overline{u}, \ \ \forall i \geq 0 \tag{27}$$

$$-\underline{\psi} \leq \psi Z(k+i+1) \leq \overline{\psi}, \forall i \geq 0 \tag{28}$$

where ψ is the matrix that gathers the state constraints. The notation $(k+i|k)$ highlights the fact that a variable at the time step $k+i$ depends on the state at the time step k, which is at each iteration the initial state of the system.

The minimax control is formulated as:

$$\min_{u(k),k\geq 0} \max_{[A,B]\in\Omega} J(k) \quad \text{with} \quad J(k) = \sum_{i=0}^{\infty} ||Z(k+i|k)||_L^2 + ||u(k+i|k)||_R^2 \tag{29}$$

s.t.

$$Z(k+i+1|k) = AZ(k+i|k) + Bu(k+i|k), \ \ \forall i \geq 0$$

with constraints:

$$-\underline{u} \leq u(k+i) \leq \overline{u}, \ \ \forall i \geq 0$$
$$-\underline{\psi} \leq \psi Z(k+i+1) \leq \overline{\psi}, \forall i \geq 0$$
$$\underline{\psi} \geq 0, \ \ \overline{\psi} \geq 0, \ \ \underline{u} \geq 0, \ \ \overline{u} \geq 0$$

4.1 New robust model predictive control strategy

Assume that after the time step $k+M$ the system is controlled using a feedback loop that will stabilize the system. We separate the optimization problem into two parts (before $k+M$ and after $k+M$) i.e. $(\Lambda) = (\Lambda_1) + (\Lambda_2)$

$$(\Lambda_1) : \text{When} \ \ 0 \leq i \leq M : \min_{u(k+i|k),k\geq 0,i=0,\cdots,M-1} \max_{[A,B]\in\Omega} J_1(k) \tag{30}$$

where,

$$J_1(k) = \sum_{i=0}^{M-1} ||Z(k+i|k)||_L^2 + ||u(k+i|k)||_R^2, \ \ i \in [0, M-1]$$

$$(\Lambda_2) : \text{When } \ i \geq M : \min_{u(k+i|k), k\geq 0, i\geq M} \max_{[A,B]\in\Omega} J_2(k) \tag{31}$$

where,

$$J_2(k) = \sum_{i=M}^{\infty} ||Z(k+i|k)||_L^2 + ||u(k+i|k)||_R^2, \ \ i \geq M$$

To get rid of the max term, we need to find convenient upper bounds to both terms of the separated cost function and that the optimal solution is the one that minimizes both upper bounds. This allows to remove the maximization term of the cost function, allowing solve the minimax optimal control problem as a minimization problem that is way easier to solve. According to Ding et at.(2004), to find an upper bound σ for J_2 that $\sigma \geq J_2(k), \ \forall [A,B] \in \Omega$ to make Λ_2 a minimization optimization by get rid of the maximum term, introduce a linear feedback control when $i \geq M$:

$$u(k+i|k) = F(k) \cdot Z(k+i|k), \ \ \forall i \geq M \tag{32}$$

To achieve this, a quadratic function is defined:

$$V(i,k) = ||Z(k+i|k)||_{P(i,k)}^2, \ \ \forall i \geq M, \ \ P(i,k) > 0 \tag{33}$$

And then impose a bound on the cost function by:

$$V(i+1,k) - V(i,k) \leq -||Z(k+i|k)||_L^2 - ||u(k+i|k)||_R^2, \ \ \forall [A,B] \in \Omega, \ \ i \geq M \tag{34}$$

By summing Equation 34 from $i = M$ to ∞, we find an upper bound to the max $J_2(k)$ term, allowing us to reformulate the minimax optimization component related to $J_2(k)$ as a problem that aims to minimize the mentioned upper bound.

$$\max_{[A,B]\in\Omega} J_2(k) \leq V(M,k) \tag{35}$$

At last, after turning the min-max optimization of $J_2(k)$ as a problem that aims to minimize the upper bound $V(M,k)$, then original min-max problem is turned into a new min-max optimization:

$$(\Lambda) : \min_{u(k+i|k), i\leq M-1, F(k), V(M,k), P(M,k) [A,B]\in\Omega} \max J(k) \tag{36}$$

where,

$$J(k) = \sum_{i=0}^{M-1} ||Z(k+i|k)||_L^2 + ||u(k+i|k)||_R^2 + ||Z(k+M|k)||_{P(M,k)}^2$$

After this transformation, the only problem is that this procedure requires turning constraints into LMI that depend on the mentioned bounds. After that, we solve this problem using toolbox CVX Research by Grant and Boyd.

4.2 Optimization

4.2.1 Without constraints

The prediction of the state Equation 14 now rewrites as:

$$\begin{bmatrix} Z(k+1|k) \\ \vdots \\ \hline Z(k+M|k) \end{bmatrix} = \begin{bmatrix} A(k) \\ \vdots \\ \hline A(k+M-1)\cdots A(k+1)A(k) \end{bmatrix} Z(k|k) + \begin{bmatrix} B(k) & 0 & \cdots & 0 \\ \vdots & \ddots & & \vdots \\ \vdots & & \ddots & 0 \\ \hline A(k+M-1)\cdots A(k+1)B(k) & & & B(k+M-1) \end{bmatrix} \begin{bmatrix} u(k|k) \\ \vdots \\ \hline u(k+M-1|k) \end{bmatrix} \tag{37}$$

or can be simplified split into above and below the dashed line, expressed as follows:

$$\begin{bmatrix} \widetilde{Z}(k+1|k) \\ Z(k+M|k) \end{bmatrix} = \begin{bmatrix} \widetilde{A}(k) \\ \widetilde{A}_M(k) \end{bmatrix} Z(k|k) + \begin{bmatrix} \widetilde{B}(k) \\ \widetilde{B}_M(k)) \end{bmatrix} \widetilde{u}(k) \tag{38}$$

Then according to the result from Equation 36, $J(k)$ changes to:

$$J(k) = ||Z(k)||^2_L + ||\widetilde{A}Z(k) + \widetilde{B}\widetilde{u}(k)||^2_{\widetilde{L}} + ||\widetilde{u}(k)||^2_{\widetilde{R}} + ||\widetilde{A}_M Z(k) + \widetilde{B}_M\widetilde{u}(k)||^2_{P(M,k)} \tag{39}$$

where $\widetilde{L}$ and $\widetilde{R}$ are:

$$\widetilde{L} = \begin{bmatrix} L & \cdots & 0 \\ \vdots & \ddots & \vdots \\ 0 & \cdots & L \end{bmatrix}, \quad \widetilde{R} = \begin{bmatrix} R & \cdots & 0 \\ \vdots & \ddots & \vdots \\ 0 & \cdots & R \end{bmatrix}$$

The uncertain parameter τ_A will take a fixed value between α and β. Let $\omega_1 = \lambda$, $\omega_2 = 1-\lambda$. There exist $l = 2$ matrices $P_l : P_1, P_2$ such that (Daafouz & Bernussou, 2001):

$$P(i|k) = \lambda P_1 + (1-\lambda)P_2, i \geq M$$

and

$$||A_l + B_l F(k)||^2_{P_t} - P_l + L + ||F(k)||^2_R \leq 0, l = 1,2\ ; t = 1,2 \tag{40}$$

[A,B] are static so $P(i|k)$ is constant for all i. Then let:

$$\gamma_1 \geq ||\widetilde{A}Z(k) + \widetilde{B}\widetilde{u}(k)||^2_{\widetilde{L}} + ||\widetilde{u}(k)||^2_{\widetilde{R}} \tag{41}$$

$$\gamma_2 \geq ||\widetilde{A}_M Z(k) + \widetilde{B}_M\widetilde{u}(k)||^2_{P(M,k)} \tag{42}$$

Combined with Equation 39, the minimax optimization problem without constrains is rewritten as a minimization problem:

$$(\Lambda) : \min_{\gamma_1,\gamma_2,\widetilde{u}(k),F(k),P_1,P_2} ||Z(k)||^2_L + \gamma_1 + \gamma_2 \qquad \text{s.t. (40) - (42)} \tag{43}$$

Now we have to transform Equations (40) - (42) into LMIs. Define that $Q_1 = \gamma_2 P_1^{-1}$, $Q_2 = \gamma_2 P_2^{-1}$ and $F(k) = YG^{-1}$, where Y is matrix of size: (number of trains)$\times$(Length of (Z)) and G is matrix of size: (Length of (Z))$\times$(Length of (Z)), where (Length of Z) = (number of trains)$\times$ $3-1$. The symbol $*$ induces a symmetric structure, so wherever $*$ is found, it should be replaced by the transposed submatrix placed in the opposite side of the diagonal of that matrix. Then the constraint Equation 40 can be transformed into the following LMI:

$$\begin{bmatrix} G+G^T-Q_l & * & * & * \\ A_lG+B_lY & Q_l & * & * \\ L^{1/2}G & 0 & \gamma_2 I & * \\ R^{1/2}Y & 0 & 0 & \gamma_2 I \end{bmatrix} \geq 0, \quad l=1,2 \tag{44}$$

And Equation 41, Equation 42 can be transform into LMIs respectively according to (Ding et al., 2004):

$$\begin{bmatrix} \widetilde{L}^{-1} & * & * \\ 0 & \widetilde{R}^{-1} & * \\ \widetilde{u}(k)^T\widetilde{B}_l^T + Z(k)^T\widetilde{A}_l^T & \widetilde{u}(k)^T & \gamma_1 \end{bmatrix} \geq 0, \quad l=1,2. \tag{45}$$

$$\begin{bmatrix} 1 & * \\ \widetilde{A}_{M,l_M}Z(k)+\widetilde{B}_{M,l_M}\widetilde{u}(k) & Q_l \end{bmatrix} \geq 0, \quad l=1,2; \quad l_M=1,2. \tag{46}$$

Now the optimization problem without constrains is rewritten as:

$$\min_{\gamma_1,\gamma_2,\widetilde{u}(k),Y,G,Q_1,Q_2} ||Z(k)||_L^2+\gamma_1+\gamma_2 \qquad \text{s.t. (44), (45) (46)} \tag{47}$$

4.2.2 With constraints

Since now the control input are parameterized by $\widetilde{u}(k)$, Equation 27 and Equation 28 can be rewritten on the basis of Equation 38 with $i=0,1,...,M-1$, which are:

$$-\underline{\widetilde{u}} \leq \widetilde{u}(k) \leq \overline{\widetilde{u}} \tag{48}$$

$$\begin{aligned} -\underline{\widetilde{\psi}} \leq \widetilde{\psi}[\widetilde{A}_lZ(k)+\widetilde{B}_l\widetilde{u}(k)] \leq \overline{\widetilde{\psi}}, \quad l=1,2; \\ -\underline{\psi} \leq \psi[\widetilde{A}_{M,l_M}Z(k)+\widetilde{B}_{M,l_M}\widetilde{u}(k)] \leq \overline{\psi}, \quad l_M=1,2 \end{aligned} \tag{49}$$

where $\underline{\widetilde{u}}$, $\overline{\widetilde{u}}$, $\underline{\widetilde{\psi}}$, $\overline{\widetilde{\psi}}$ and $\widetilde{\psi}$ are vectors constructed using the same rule as Equation 38. According to Cuzzola et al. (2002), assume that there exist two symmetric matrices $Q_l=P_l^{-1}>0$, $l=1,2$, two symmetric matrices $\{\Phi,\Gamma\}$ and a set of matrices $\{G,Y\}$ satisfying following:

$$\begin{bmatrix} \Phi & Y \\ Y^T & G+G^T-Q_l \end{bmatrix} \geq 0, \quad \Phi_{jj} \leq \phi_{j,inf}^2, \quad l=1,2, \quad j=1,2,...,m \tag{50}$$

$$\begin{bmatrix} G+G^T-Q_l & * \\ \psi(A_lG+B_lY) & \Gamma \end{bmatrix} \geq 0, \quad \Gamma_{ss} \leq \psi_{s,inf}^2, \quad l=1,2; \quad s=1,2,...,q \tag{51}$$

where $\phi_{j,inf}=\min\left\{\underline{u}_j\overline{u}_j\right\}$, $\psi_{s,inf}=\min\left\{\underline{\psi}_s,\overline{\psi}_s\right\}$ and Φ_{jj} is the jth diagonal element of Φ, Γ_{ss} is the sth diagonal element of Γ.

The entire optimization problem is now expressed as a minimization problem subject to several LMIs:

$$\min_{\gamma_1,\gamma_2,\widetilde{u}(k),Y,G,Q_1,Q_2} ||Z(k)||_L^2+\gamma_1+\gamma_2 \qquad \text{s.t. (44), (45), (46), (48), (49), (50) and (51)} \tag{52}$$

When solving this optimization problem, we give the initial state Z(k|k) and apply the calculated optimal control u(k|k) in order to drive the system to Z(k+1|k). After this, take then $k+1$ as the new initial time step of system and repeat this iterative process.

5 Simulation result

In this section, we declared the parameter setting, explained simulation and tuning process, and the result.

5.1 Parameter settings

We define a platoon consisting of four trains, which contains a leader train and N = 3 followers. We consider a homogeneous fleet, that is to say, τ^A takes the same fixed (but unknown) value for all the considered trains. The desired time gap between trains is set as 1 s. For trains, $l_n = 100m, \forall n$, $v_{ref} = 110km/h$, $v_{max} = 150km/h$ and the acceleration is between -1 m/s^2 and 1 m/s^2. For the controller, $\Delta t = 2s$, $t^d = 1s$, $s_{min} = 5m$. The actuator lag $\tau^A \in [0.5s, 1s]$ and the total control time is 180 s. In the initial state of the fleet, all trains travel at a constant speed equal to 110km/h with distance gaps of 200 m, and the controller virtually couples these trains into a platoon, and the leading train tries to track the reference speed. (target speed).

5.2 Control performance for different weights

The weight parameters are manually tuned to find out the best controller performance weight allocation, to get the impact of weights on performance, the shortest actuator lag is chosen to reduce the impact of lag time (when $\tau^A = 0.5s$). First, we chose to make each of the four weight parameters much larger than the other three to evaluate the impact of each weight on controller performance, the parameter values per experiment is shown in Table 1.

Table 1: Parameter values for four scenario

Scenario	Safety weight (c_1)	Stability weight (c_2)	Comfort weight (c_3)	Energy consumed weight (c_4)
Penalizing the performance term of the cost	10	0.01	0.01	0.01
Penalizing the platoon stability term	0.01	10	0.01	0.01
Penalizing the comfort term	0.01	0.01	10	0.01
Penalizing the energy consumption term	0.01	0.01	0.01	10

- **Penalizing the performance term of the cost**

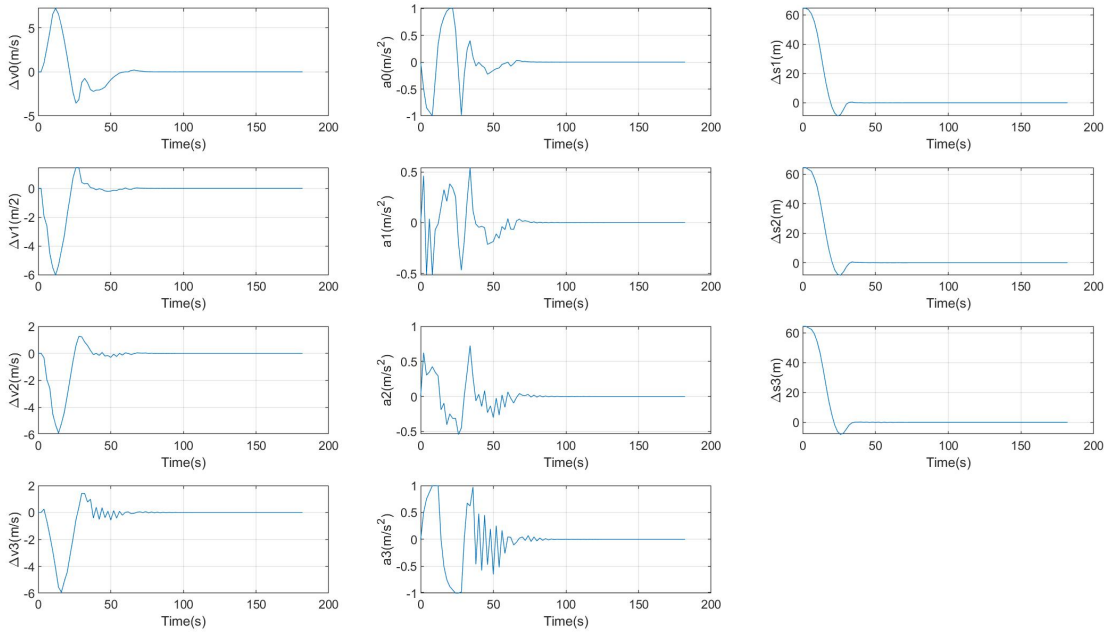

Figure 2: Relative speed, acceleration and distance gap error for each train when performance term is penalized

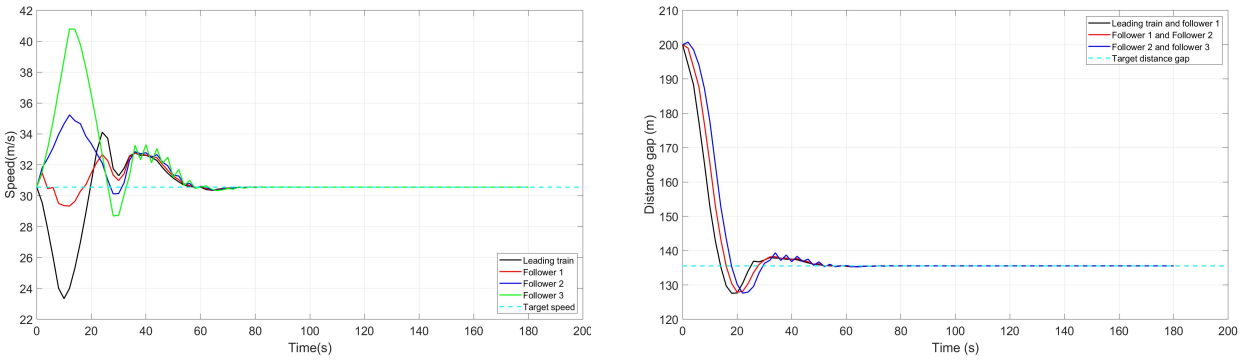

(a) Actual speed

(b) Actual distance gap

Figure 3: Actual speed and distance gap when performance term is penalized

When penalizing the performance term of the cost, controller minimized the distance gap error which are aimed at make distance gap to reach the desired distance gap quickly. From Figure 2 and Figure 3, although the platoon complete the virtual coupling in a very short time, the changes in train speed and acceleration exhibited extremely volatile fluctuations that could not have occurred in real operation. Also, to complete the coupling faster, the leading train and the last follower fluctuate greatly in speed and the third follower even has frequent acceleration and deceleration in a short period of time. So, the controller fails to provide a convenient control strategy when penalizing the performance over the other terms of the cost function.

- **Penalizing the platoon stability term**

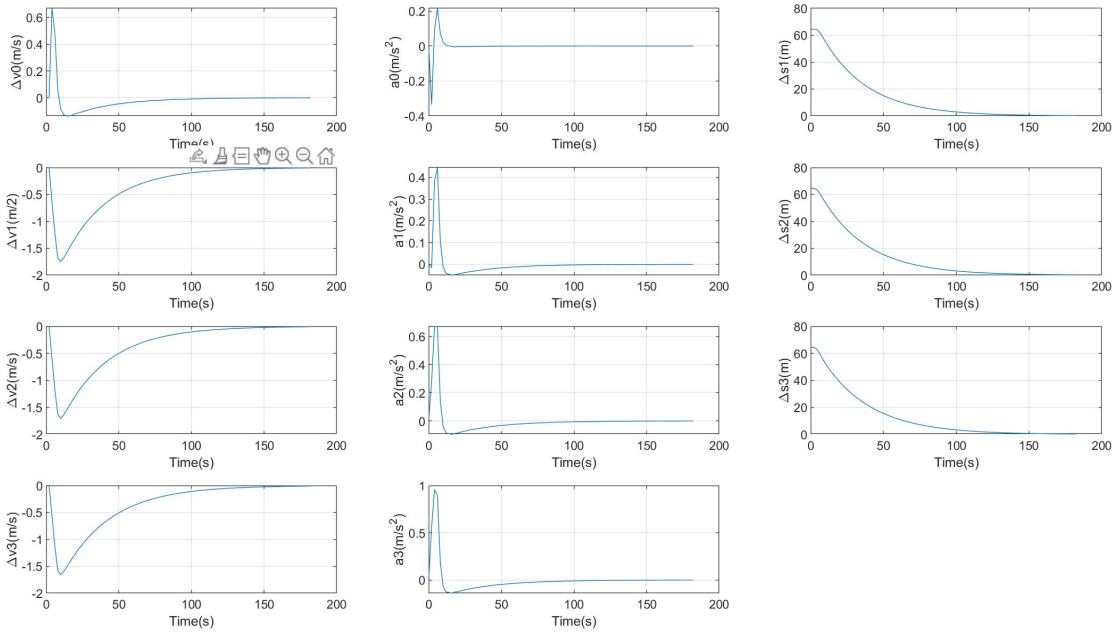

Figure 4: Relative speed, acceleration and distance gap error for each train when penalizing the platoon stability

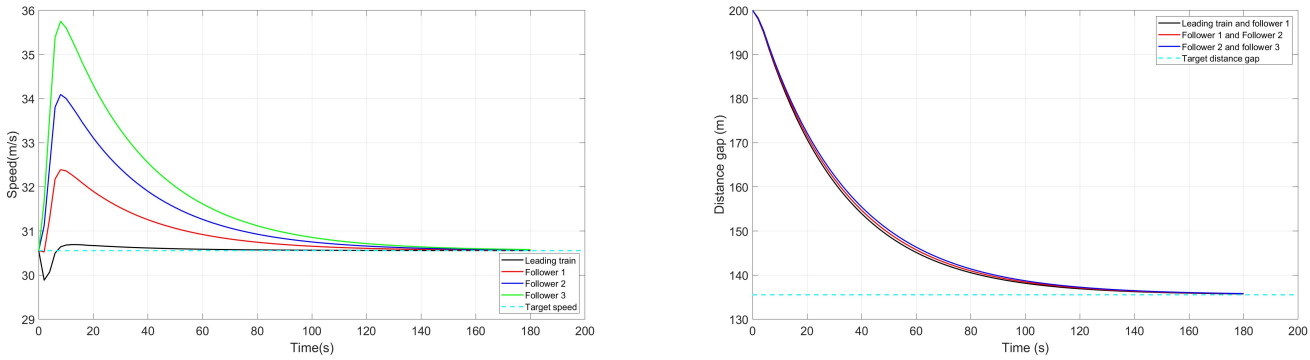

(a) Actual speed

(b) Actual distance gap

Figure 5: Actual speed and distance gap when penalizing the platoon stability

The stability parameter makes the speed difference between trains smaller, and it can be seen from Figure 5 that the entire virtual coupling process has only experienced one acceleration process and one deceleration process, and the three followers gradually move closer to the leading train by accelerating first and then slowly decelerating. The whole coupling process shows that the speed of the leading train changes very little, and the followers gradually move closer to the leader. This smoother virtual coupling is also needed in actual railway transportation operations. However, due to the long deceleration process, the virtual coupling time reached about 100 seconds.

- **Penalizing the comfort term**

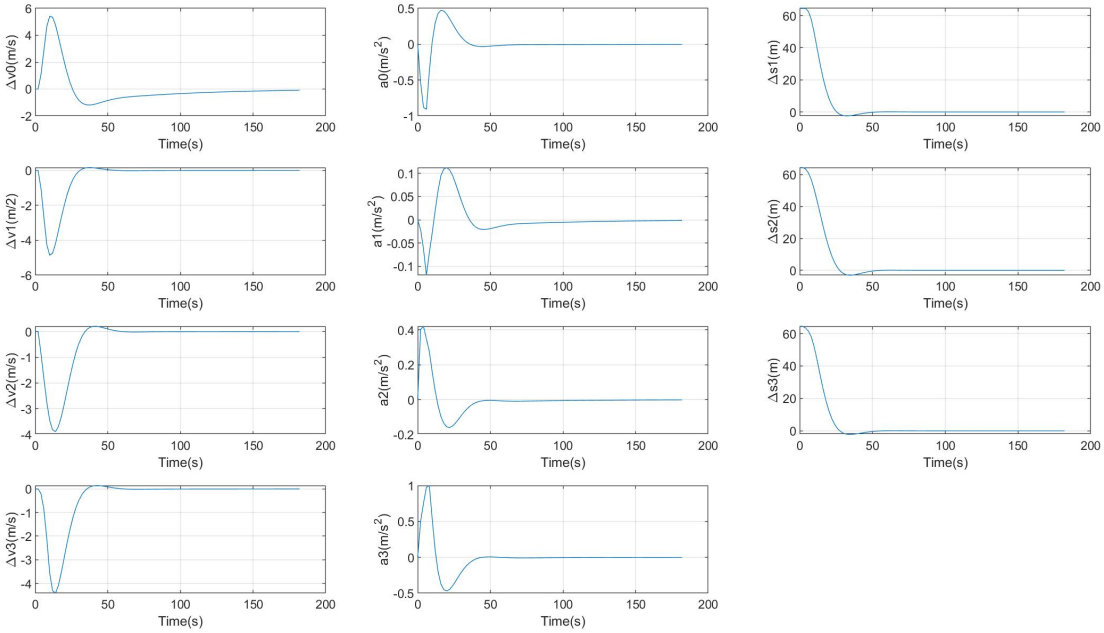

Figure 6: Relative speed, acceleration and distance gap error for each train when penalizing the comfort term

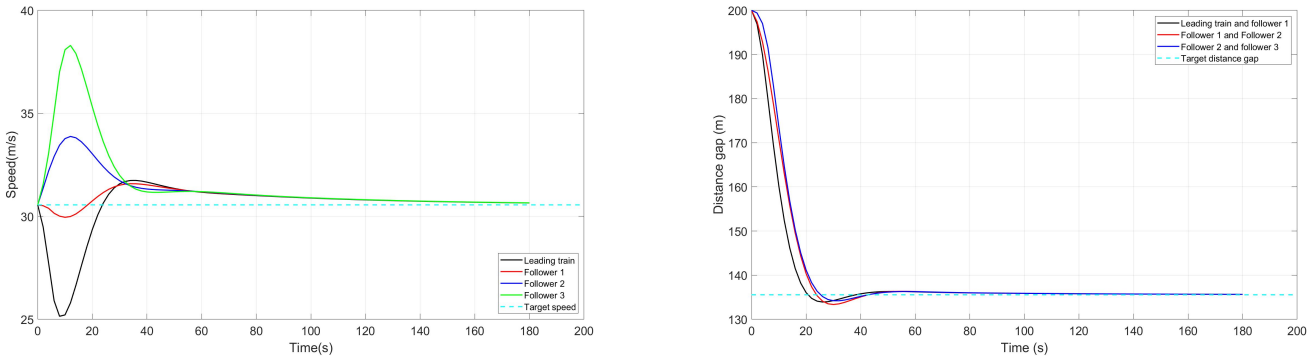

(a) Actual speed

(b) Actual distance gap

Figure 7: Actual speed and distance gap when penalizing the comfort term

- **Penalizing the energy consumption term**

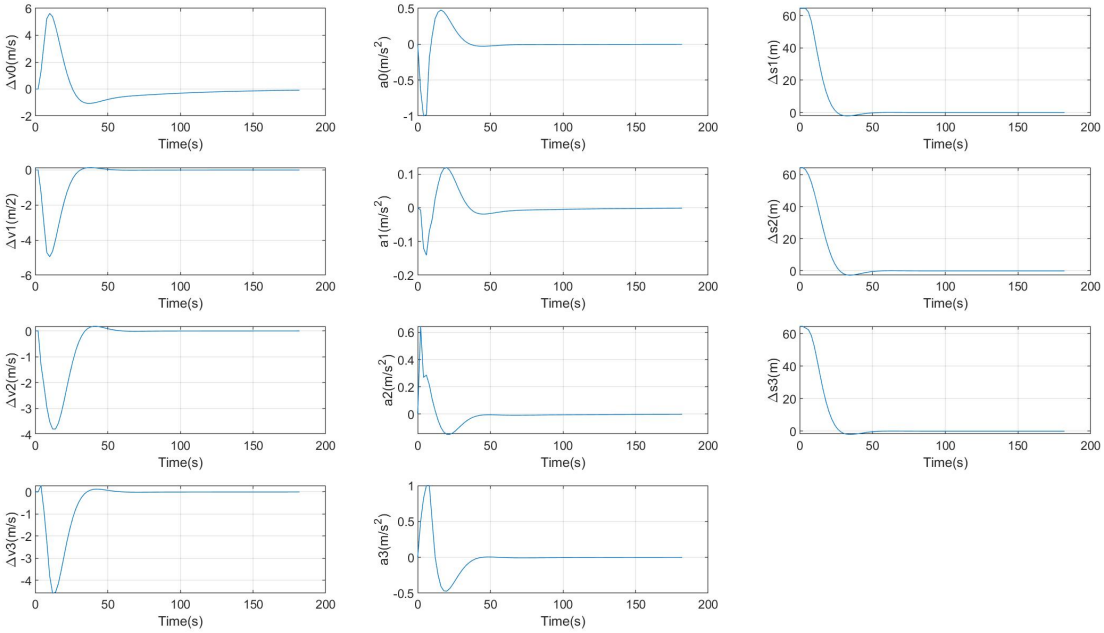

Figure 8: Relative speed, acceleration and distance gap error for each train when penalizing the energy consumption term

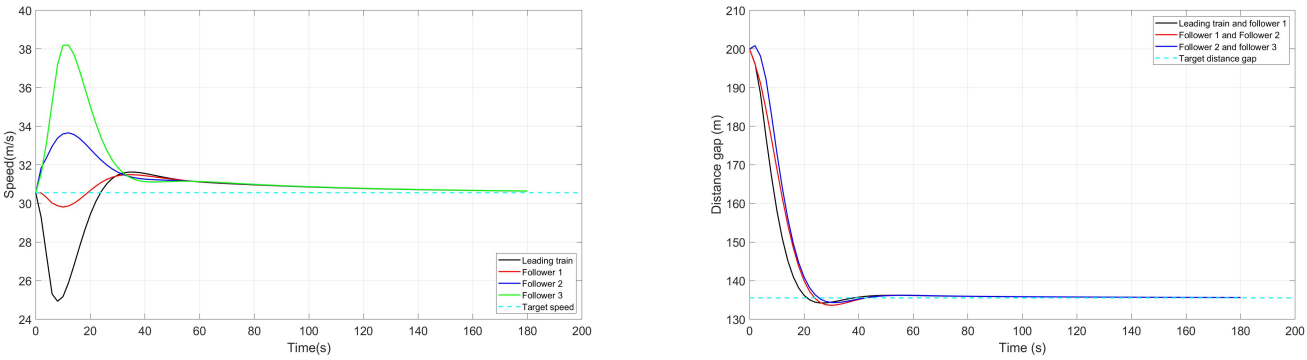

(a) Actual speed

(b) Actual distance gap

Figure 9: Actual speed and distance gap when penalizing the energy consumption term

Both the comfort weight and the energy consumption weight are acceleration-related parameters and therefore exhibit similar performance. At the beginning of the virtual coupling, there is a large difference in speed between different vehicles, and because these two parameters make acceleration tends to 0, the entire virtual coupling process takes longer to reduce the speed to target speed. So in a short period of time, the speed of the train converged to the same but did not reach the target speed, and with a small acceleration limit, they took longer to complete the virtual coupling.

Table 2: Maximum relative speed, maximum acceleration vary with weight parameters tuning

c_1	Max Δv (m/s)	Max acceleration (m/s^2)
0.010	1.95	0.791
0.011	2.03	0.838
0.012	2.10	0.862
0.013	2.14	0.855
0.014	2.19	0.849
0.015	2.24	0.842
0.016	2.29	0.839
0.017	2.33	0.834
0.018	2.38	0.828
0.019	2.47	0.862
0.020	2.37	0.886

5.3 Controller optimization

Since penalizing the stability shows an adequate but slow control performance, we fix the weight related to the stability term and vary the performance one to accelerate the process. We decided to give the fixed values for the other $c_i, i = 2, 3, 4$ under the worst case (τ^A= 1s) and tuning the value of performance weight (c_1) to shorter the converge time to get the optimal control performance.

Because the output starts to show slight fluctuations when the performance parameters reach 0.02, we choose to look for the optimal results from 0.01-0.02. As shown in Table 2, the relative speed does not show a significant change when tuning. In order to make the train acceleration as small as possible to ensure the comfort of train operation and the stability of virtual coupling, Figure 10 shows that when performance parameter equal to 0.018, controller reduces the convergence time while maintaining a small maximum acceleration.

The optimal result under the worst case shown in Figure 12, Compared to the result that only penalizes stability term (Figure 11), the optimal result reduces the convergence time by about 20 seconds while ensuring a smooth virtual coupling process.

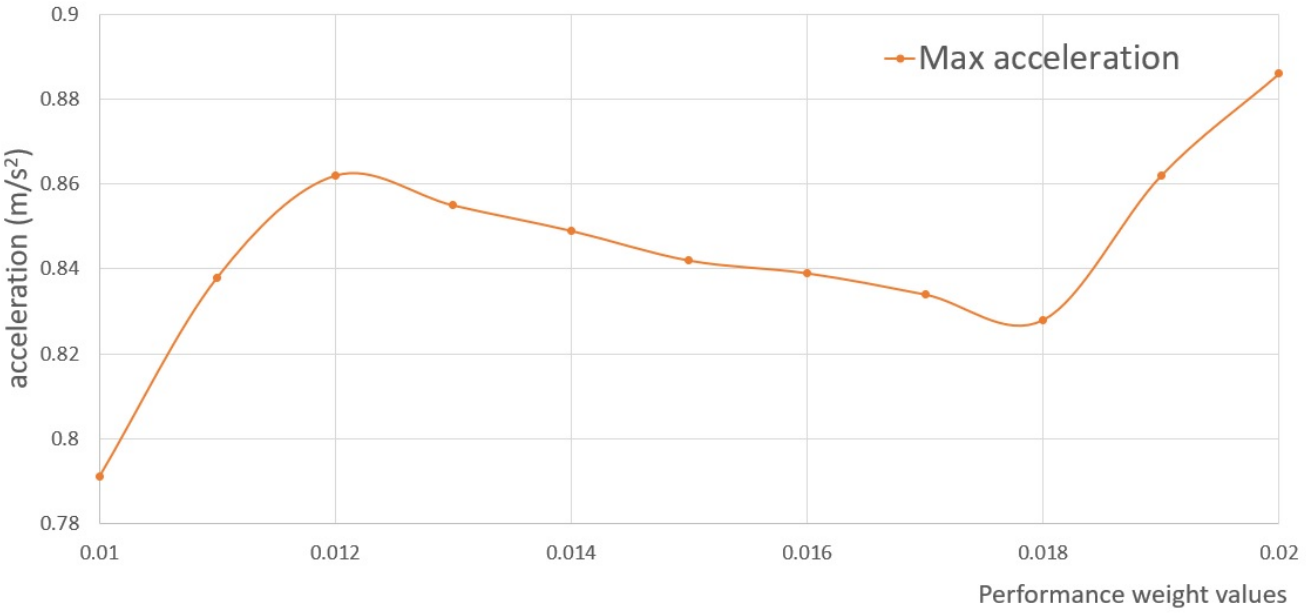

Figure 10: Maximum acceleration vary with weight tuning

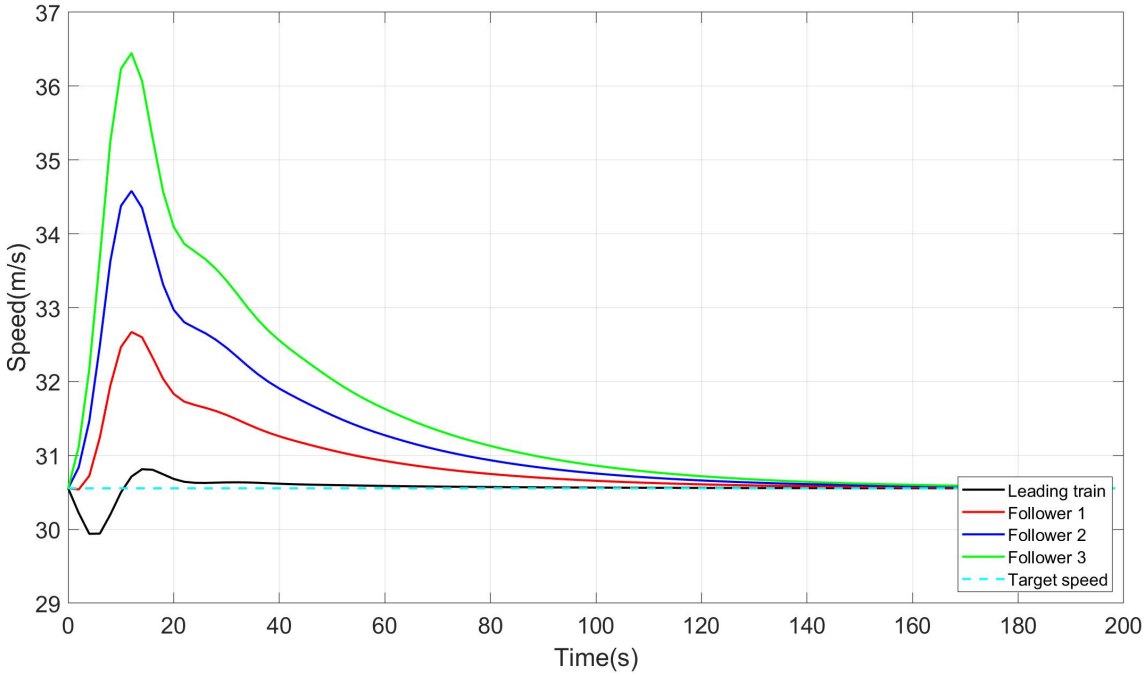

Figure 11: Actual speed when penalized stability term
($\tau^A = 1s, c_1 = 0.01, c_2 = 10, c_3 = 0.01, c_4 = 0.01$)

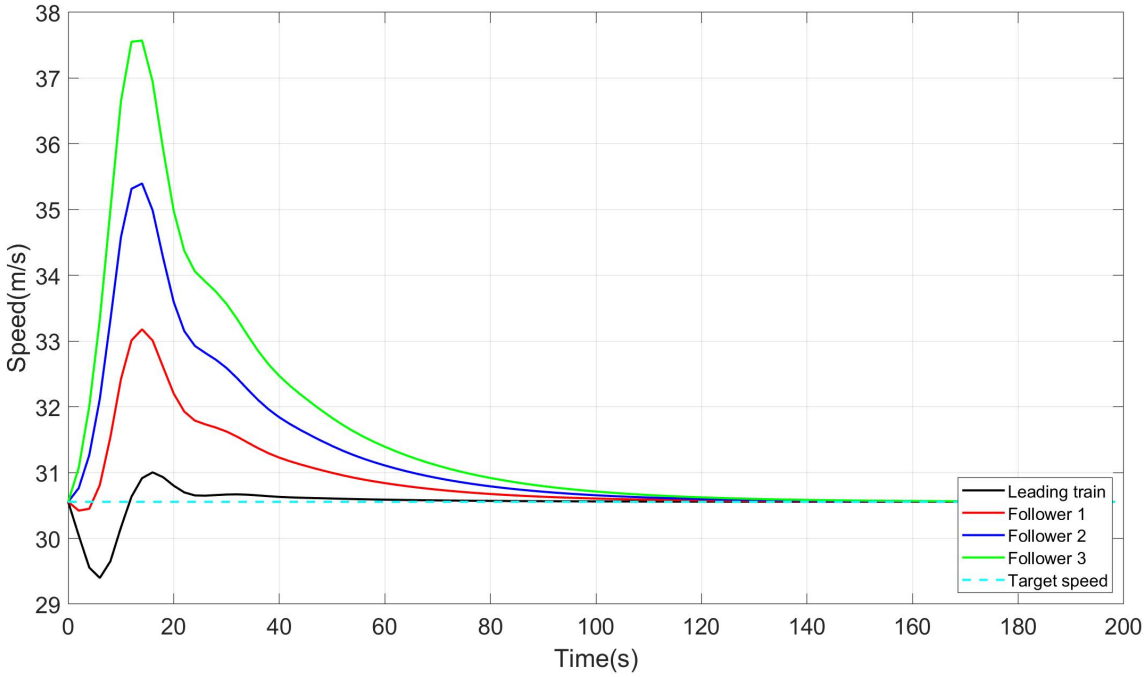

Figure 12: Actual speed under optimal control condition
($\tau^A = 1s, c_1 = 0.018, c_2 = 10, c_3 = 0.01, c_4 = 0.01$)

5.4 Sensitivity analysis

A sensitivity analysis of controller has been carried out to investigate the influence of different actuator lag on performances of virtual coupling.

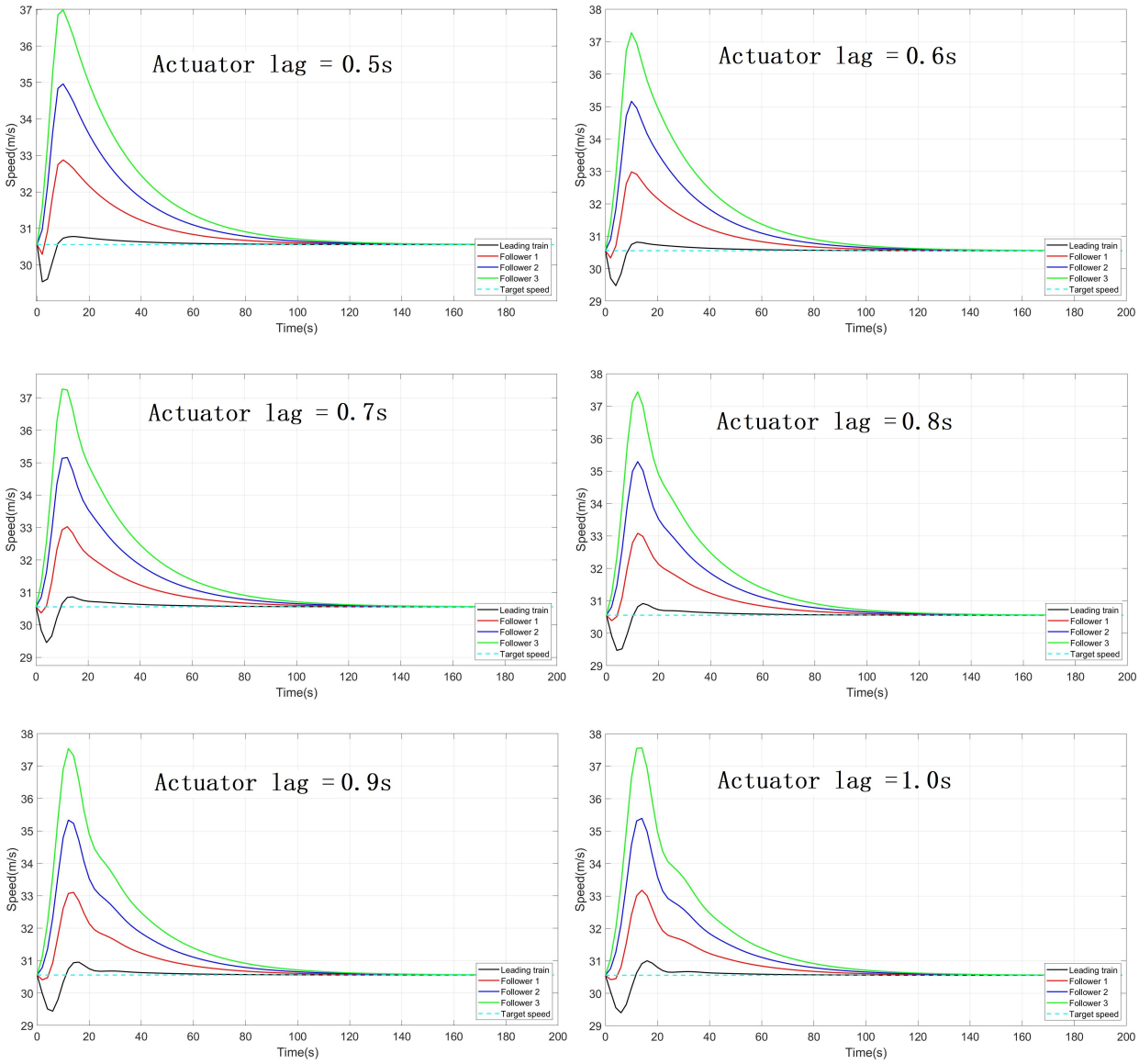

Figure 13: Actual speed when $\tau^A \in [0.5s, 1.0s]$ $(c_1 = 0.018, c_2 = 10, c_3 = 0.01, c_4 = 0.01)$

The sensitivity results show that change of actuator lag does have an impact on the performance of the controller, mainly when the speed changes gradually become slightly fluctuating. First, the maximum speed of all trains has increased slightly, and the leading train shows slight fluctuations from scratch to accommodate this speed increase. Although the maximum speed varied, this did not affect the convergence time of the virtual coupling, and the controller adjusted the deceleration process so that the convergence time in each experiment was almost the same which still around 80 seconds. So, the result is actuator lag within the acceptable range will not significantly affect the normal operation of the controller.

6 Conclusion and recommendation

This paper proposed a robust model predictive control for a train platoon. We formulate the robust control problem as a minimax MPC which in turn is reformulated as a minimization problem subject to LMIs, which is the problem that is solved in this paper to calculate the robust-optimal control policy. Through simulation, the impact of four weights, including safety, platoon stability, comfort and energy consumed, on the controller was discussed. Through the tuning of the weight parameters, we found that penalizing the stability of the platoon led to a control strategy that had an appropriate performance. On this basis, by adjusting the safety weight parameter, the time required for virtual coupling is greatly reduced, which can make controller efficiently and safely completes the virtual coupling of the train platoon. In the sensitivity analysis, the flexibility of the model is verified, and the train control within the actuator lag range can be completed. This robustness to lag times can improve the efficiency of train virtual coupling, which may have a positive impact on railway operation and capacity of rail traffic.

This controller also has some limitations. First of all, the control process is to couple several trains running smoothly into a platoon. In this process, whether the leading train might have other heterogeneous behaviors is not considered, because the leading train and follower are controlled together. The second point, this linear system is a simple model, controlling the acceleration of the train by traction and braking force was not realized. Also in our assumption, the track is straight and flat, some of the effects of turning behaviour and track gradient are not considered in the model so the model can not realize online implementation so far. Finally, the calculation time of each time step of this model is about 2.75 seconds, but one time step is 2 seconds, which means that there is a time gap of 0.75 seconds, which makes it hard to calculate the next behavior of the train in time and transmit it to the operating system. Perhaps a more advanced on-board equipment is required to complete the calculation or further simplification of the calculation process is required. However, despite not being suitable for an online implementation, the framework presented here constitutes an initial step towards virtual coupling platoon formation under uncertainty.

References

A. Cuzzola, F., C. Geromel, J., & Morari, M. (2002). An improved approach for constrained robust model predictive control. *Automatica*, *38*(7), 1183-1189.

Barney, D., Haley, D., & Nikandros, G. (2001). Calculating train braking distance. In *Conferences in research and practice in information technology series* (Vol. 146, pp. 23–29).

Chen, N., Wang, M., Alkim, T., & Van Arem, B. (2018). A robust longitudinal control strategy of platoons under model uncertainties and time delays. *Journal of Advanced Transportation*, *2018*, 13.

Daafouz, J., & Bernussou, J. (2001). Parameter dependent lyapunov functions for discrete time systems with time varying parametric uncertainties. *Systems & control letters*, *43*(5), 355–359.

Di Meo, C., Di Vaio, M., Flammini, F., Nardone, R., Santini, S., & Vittorini, V. (2019). Ertms/etcs virtual coupling: proof of concept and numerical analysis. *IEEE Transactions on Intelligent Transportation Systems*, *21*(6), 2545–2556.

Ding, B., Xi, Y., & Li, S. (2004). A synthesis approach of on-line constrained robust model predictive control. *Automatica*, *40*(1), 163–167.

Felez, J., Kim, Y., & Borrelli, F. (2019). A model predictive control approach for virtual coupling in railways. *IEEE Transactions on Intelligent Transportation Systems*, *20*(7), 2728–2739.

Grant, M., & Boyd, S. (2008). Graph implementations for nonsmooth convex programs. In V. Blondel, S. Boyd, & H. Kimura (Eds.), *Recent advances in learning and control* (pp. 95–110). Springer-Verlag Limited.

Park, J., Lee, B.-H., & Eun, Y. (2022). Virtual coupling of railway vehicles: Gap reference for merge and separation, robust control, and position measurement. *IEEE Transactions on Intelligent Transportation Systems*, *23*(2), 1085-1096.

Quaglietta, E. (2019). Analysis of platooning train operations under v2v communication-based signaling: Fundamental modelling and capacity impacts of virtual coupling. In *Proceedings of the 98th Transportation Research Board Annual Meeting* .

Quaglietta, E., Spartalis, P., Wang, M., Goverde, R. M. P., & van Koningsbruggen, P. (2022). Modelling and analysis of virtual coupling with dynamic safety margin considering risk factors in railway operations. *Journal of Rail Transport Planning & Management*, *22*, 100313.

Quaglietta, E., Wang, M., & Goverde, R. M. P. (2020). A multi-state train-following model for the analysis of virtual coupling railway operations. *Journal of Rail Transport Planning & Management*, *15*, 100195.

Zhang, X., Yang, D., Zhang, W., & Huang, J. (2022). Optimal robust constraints-following control for rail vehicle virtual coupling. *Journal of Vibration and Control*.